Progress In Electromagnetics Research Letters, Vol. 82, 121–128, 2019

Suppression of Higher Order Modes of a Two Element Microstrip Array Using Open-Ended Stubs

Susmita Biswas[1, *], Chandan K. Ghosh[2], Santimoy Mandal[3], Goffar A. Sarkar[4], Soumen Banerjee[5], and Durbadal Mandal[1]

Abstract—In this paper suppression of higher order modes of a microstrip antenna array is investigated. The array consists of two radiating elements which are fed by a corporate type microstrip feeding network. The array provides resonance at 5.2 GHz frequency for its fundamental mode (TM_{10} mode). Beside this fundamental mode, two harmonics at 10.4 GHz (1st harmonic) and 15.05 GHz (2nd harmonic) and a few sub-harmonics at 7.8 GHz (TM_{01}), 8.8 GHz (TM_{11}), and 13.3 GHz (TM_{12}) are excited. In order to suppress the 1st harmonics, a pair of half wavelength open ended stubs whereas for 2nd harmonic a pair of quarter wavelength open ended stubs are employed. From the simulated results it has been noticed that the 1st and 2nd harmonics are successfully suppressed, and the sub-harmonics are also suppressed. Prototypes of the antenna arrays are fabricated and measured. Measured results have good agreement with simulated ones.

1. INTRODUCTION

Microstrip antennas are widely used in wireless communication systems because of their advantageous features such as light weight, low volume, and easy fabrication. However, they suffer from excess harmonic radiation which degrades the overall system performance [1]. It is needed to have low level of radiation at harmonic frequencies for better performance of the systems. Generally, this is achieved by introducing additional filter circuits within the antenna system. But this is not a suitable solution as this makes the antenna system bulky. To overcome this problem, Horii and Tsutsumi first experimentally demonstrated the control of higher order modes with the use of Photonic Band Gap (PBG) structures in 1999. Circular holes were etched out on the ground plane underneath the patch, and unwanted harmonics were suppressed due to the stop-band characteristic of the PBG structure [2]. Electromagnetic Band Gap (EBG) structures have also been used in many works to suppress the harmonics. In [3], EBG structures are used in slotted microstrip patch antenna to realize significant suppression of harmonics. Biswas et al. controlled the radiations at higher harmonics by partial ring shape Defected Ground Structure (DGS) [4]. In [5], the author presented harmonic suppression using open ended stubs in a single element antenna. In this case, the 1st and sub-harmonics are eliminated by using two stubs of quarter wavelength on both sides of the microstrip feed line. Recently, a hexagon-shaped DGS structure is implemented to suppress higher-order modes [6]. Extensive work on harmonic suppression has been carried out on single element antennas until the present. There are very few works available in the literature so far on harmonic reduction in an antenna array [7–9] though it is very much needed for high gain and long-distance communication. 2D EBG structure and dumbbell-shaped DGS are used in [7] and [8] respectively to suppress higher order harmonics. In [9], a rectangle-shaped

Received 21 November 2018, Accepted 1 March 2019, Scheduled 18 March 2019
* Corresponding author: Susmita Biswas (susmitabiswas404@gmail.com).
[1] Department of ECE, National Institute of Technology, Durgapur, India. [2] Department of ECE, Dr. B. C. Roy Engineering College, Durgapur, India. [3] Dept. of ECE, R.V.S. College of Engineering & Technology, Jharkhand, India. [4] Indian Institute of Engineering Science and Technology, Howrah, India. [5] Department of ECE, University of Engineering & Management, Kolkata, India.

DGS has been used in two element antenna arrays to suppress higher order modes. In [10], a novel dual planar electromagnetic bandgap (DP-EBG) microstrip structure is investigated to suppress the spurious radiation of the patch antenna. As per the authors' knowledge, there is no work on harmonic suppression using open ended stub in an array. Abbasiniazare et al. in [11] exhibited an excellent work on Mutual Coupling Compensation using Split-Ring Resonators. In this work, the authors have used split-ring resonators and tackled mutual coupling between the helical antenna elements without affecting the basic antenna parameters such as gain, S-parameters, and antenna efficiency.

In this paper, the authors explore a technique to reduce higher order modes of a two-element array by using only open-ended stubs. As the stubs are printed on the same side of the radiating elements, there is no scope of back radiation as presented in the case of EBG and DGS structures. Two pairs of stubs are placed on both sides of the feed line of the array. The implementation of these stubs efficiently suppress the harmonics and sub-harmonics. The structure is designed and simulated by IE3D electromagnetic simulator. The proposed optimum topology is used for wireless power transfer to improve the RF/Microwave front-end sub-system and suitable for energy scavenging. The patch with harmonic suppression can be used in rectenna system, WLAN or wearable energy application where it provides system size reduction. The proposed new idea to suppress harmonics can improve the overall system performance by maximizing the power transfer at fundamental frequency for wearable energy application and rectenna system in wireless application. The resonance frequency of antenna array is 5.2 GHz. The lower and upper cutoff frequencies are 5.0 GHz and 5.6 GHz with a bandwidth of 0.6 GHz.

2. STUB INTEGRATED ANTENNA ARRAY

Figure 1 shows the configuration of the proposed antenna array. The antenna array is designed on an FR4 substrate of thickness 1.58 mm, dielectric constant of 4.4, and loss tangent of 0.02. This array consists of two radiating elements (patch) which have resonance at 5.2 GHz. The width (a) and length (b) of the patches are calculated using the standard design formula of microstrip patch antenna [12], which is further optimized to get the desired responses. The patches are excited by a microstrip feed network which is defined by parameters 'e', 'f', 'i' and 'j'. Two pairs of open-ended stubs (pair of stub A and pair of stub B) are integrated with the array, and their larger views are shown in Fig. 2. Stub 'A' is defined by 'k', 'm', 'n', and 'o' whereas stub 'B' is defined by parameters 'p', 'q', 'r', and 's'. All the dimensions are listed in Table 1. The antenna is fed by a vertical 50 Ohms transmission line which is further divided into two 100 Ohms horizontal lines as shown in Fig. 1. These 100 ohms lines are fed to patch elements of the array.

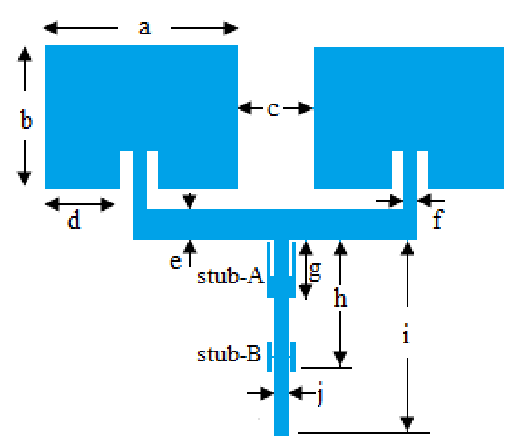

Figure 1. Structure of the proposed antenna array.

Rectangular microstrip patch array and its equivalent circuit transmission-line model has been designed. The general topology of the stub integrated array equivalent circuit is shown in Fig. 2(c). Each radiating slot of the microstrip patch is represented by parallel capacitance and resistance. The stub is represented by series capacitance and inductance.

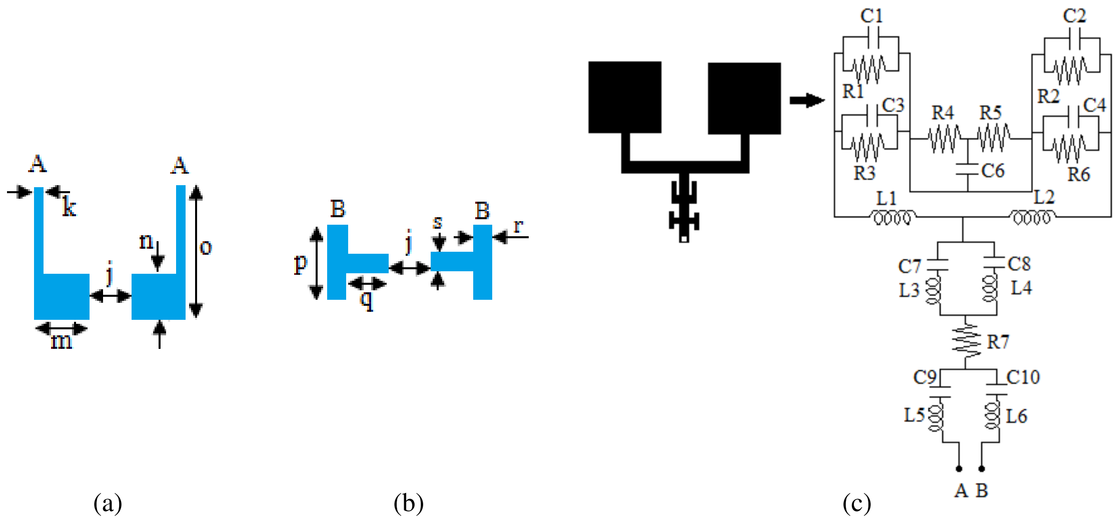

Figure 2. (a) Stub 'A' of vertical length (o) $\approx \lambda_{g1}/2$ ($\lambda_{g1} \approx$ guided wavelength of the 1st harmonic frequency and (b) Stub 'B' of vertical length (p) $\approx \lambda_{g2}/4$ ($\lambda_{g2} \approx$ guided wavelength of 2nd harmonic frequency. (c) Equivalent circuit of stub integrated array.

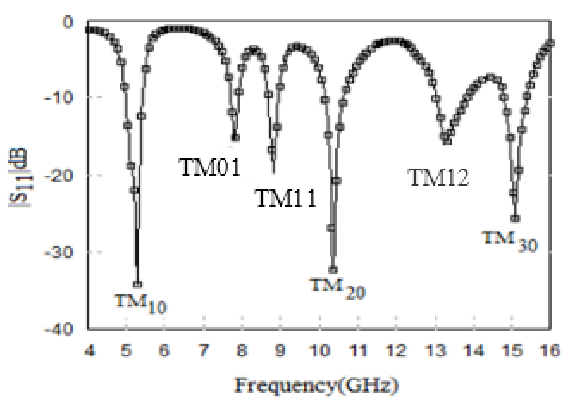

Figure 3. Simulated $|S_{11}|$ characteristic of the reference array.

Table 1. Antenna and stub dimensions (in mm).

Parameters	a	b	c	d	e	f
Dimension	17.5	13.1	13.8	7.2	2.6	1.4
Parameters	g	h	s	i	j	k
Dimension	6.8	13.325	0.2	20.275	2.025	0.325
Parameters	m	n	o	p	q	r
Dimension	0.6	3.525	6.75	2.425	0.2	0.5

The antenna array is designed and simulated in two steps: i) without stubs and ii) with stubs. The simulated input reflection coefficient of the array without stubs is shown in Fig. 3. The figure reflects the presence of harmonics (TM_{20} and TM_{30} modes) and sub-harmonic (TM_{12}, TM_{22}, and TM_{32} modes) [4] along with the fundamental frequency (TM_{10} mode). To suppress the harmonics and sub-harmonics, two pairs of stubs (stub pair A and stub pair B) are integrated with the feed line. The vertical length of stub 'A' is chosen to be half of the guided wavelength of the 1st harmonic ($\lambda_{g1}/2$) whereas the same

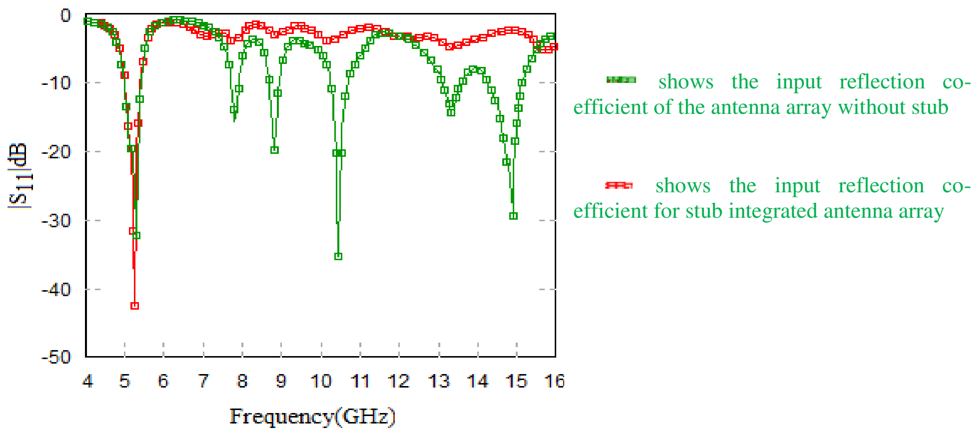

Figure 4. Simulated $|S_{11}|$ characteristic of the reference array and the stub integrated array.

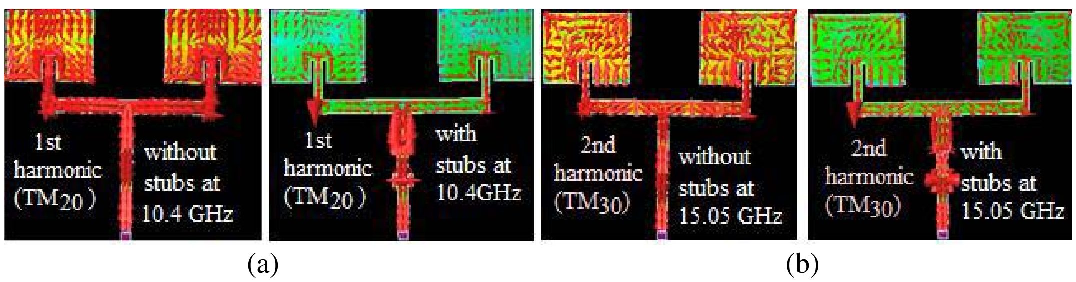

Figure 5. Simulated current distribution (a) at 10.4 GHz and (b) at 15.05 GHz. (from left without stubs and with stubs).

is chosen for stub 'B' as quarter of the guided wavelength of the 2nd harmonic ($\lambda_{g2}/4$) to suppress the corresponding harmonics. The simulated $|S_{11}|$ of the array with stubs and the array without stubs are shown Fig. 4. Effective suppression of the 1st and 2nd harmonics along with sub-harmonics is evident from this figure. The 1st harmonic is suppressed due to stub pair 'A' and that for 2nd harmonic is due to stub pair 'B' as their vertical length is half and quarter wavelength of the corresponding harmonic frequency, respectively. The simulated current distributions at 10.4 and 15.05 GHz frequencies are shown for both the cases (without stubs and with stubs) in Fig. 5(a) and Fig. 5(b), respectively. It is noticed from Fig. 5(a) that the surface current flow on the patch decreases at the 1st harmonic (10.4 GHz) when stubs are integrated compared to without stubs. The reduction of surface current flow on patch is due to large accumulation of current at stub pair 'A'. This reduction of current flow on the patch effectively suppressed the 1st harmonic. In the same way from Fig. 5(b), the suppression of the 2nd harmonic can be explained. Furthermore, due to the combined effect of both stubs, the sub-harmonics also get suppressed. Normally, the stub has a stopband and passband. In this work, we set the passband and stopband in such a way that it passes the fundamental frequency and stops the higher order modes of propagation. The stopband and passband of the stub have been optimized by the process of simulation, and it has been observed that there is no change of the antenna characteristics after the introduction of stub (optimized). Moreover, different lengths of stub provide different stopbands and passbands. So, by using the same set of stubs different stopbands and passbands cannot be achieved.

The radiation simulated patterns of the array using stub pair 'A' and pair 'B' and that without stubs are shown in Fig. 6 for fundamental frequency (f_0) as well as harmonic frequencies ((f_1 and f_2). From the figure it is observed that the co-polar radiation pattern at 5.2 GHz frequency has the same nature (as like without stubs) after stubs integration. The simulated current distributions for both the cases at fundamental frequency are shown in Fig. 6(b) and find that the surface current distribution remains almost unchanged after stubs integration. The unchanged surface current distribution reveals

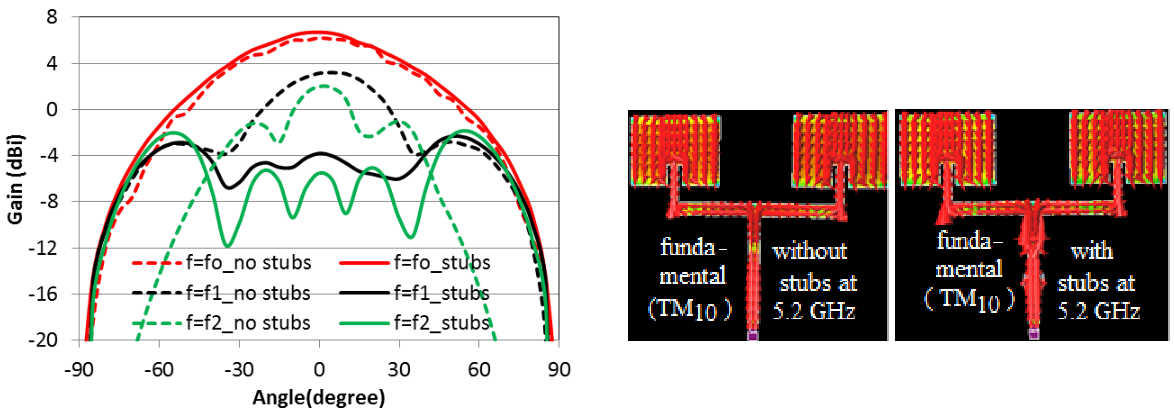

(a) (b)

Figure 6. (a) Simulated elevation pattern views (co-pol.) of the array [f_0 = fundamental, f_1 = 1st harmonic and f_2 = 2nd harmonic]. (b) Surface current distribution at 5.2 GHz (from left without stubs and with stubs).

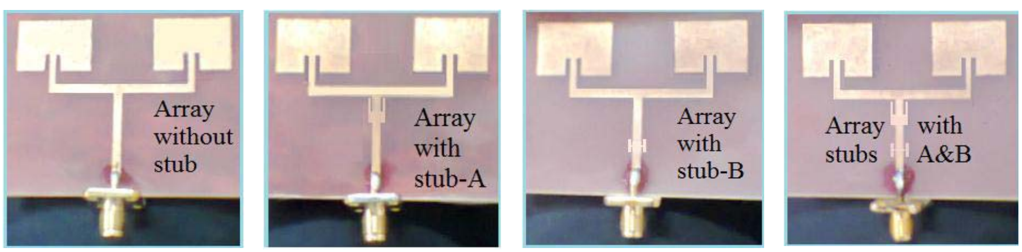

(a) (b) (c) (d)

Figure 7. Fabricated antennas (a) without stubs (b) with stub-A (c) with stub-B and (d) with both stubs.

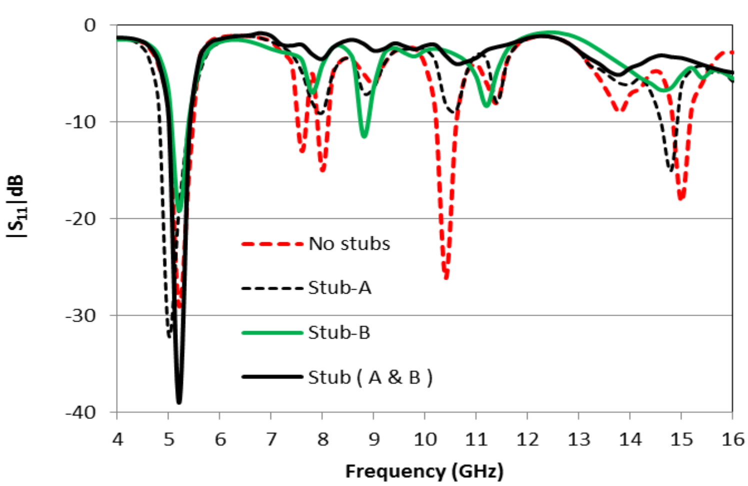

Figure 8. Measured $|S_{11}|$ characteristics of the array for different configurations.

the reason for the same nature of radiation patterns at fundamental frequency for both the cases (without stubs and with stubs). The radiations for harmonic frequencies 10.4 GHz and 15.05 GHz get reduced by 7.5 dB and 8.0 dB, respectively.

3. PROTOTYPE OF THE ARRAYS AND MEASURED RESULTS

The reference antenna array and the arrays with different combinations of stubs (only stub pair 'A', only stub pair 'B', and both stub pairs) are fabricated with an FR4 substrate, and the fabricated antenna prototypes are shown in Fig. 7. $|S_{11}|$ of these antenna arrays are measured using an N5230A network analyser. The measured $|S_{11}|$ for the arrays with different combinations of stub pairs are shown in Fig. 8. The $|S_{11}|$ with stub pairs is as the simulated one, which reveals the suppression of harmonics and sub-harmonics.

The measured 2D co-polar radiation patterns of the reference antenna array and the array with both pairs of stubs for fundamental and harmonic frequencies are depicted in Fig. 9. It is noticed that the peak gains at the 1st and 2nd harmonic frequencies are reduced by 5.5 dBi and 6 dBi, respectively. It is also observed that the measured radiation patterns differ from simulated ones by 2 dBi for the 1st and 2nd harmonics. This small discrepancy in measured result is observed due to manual fabrication.

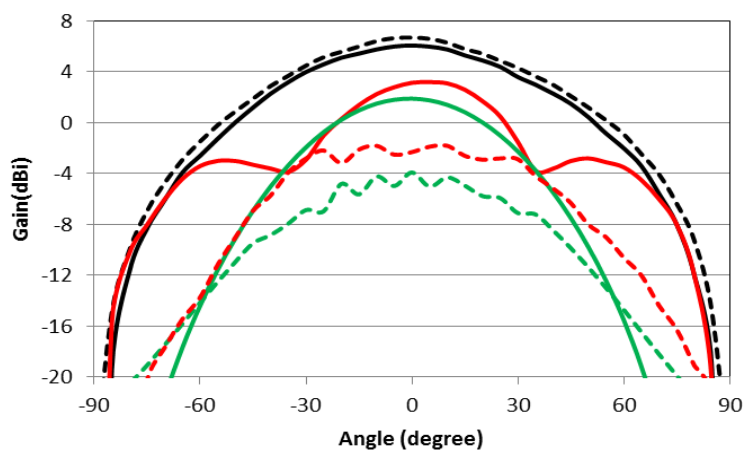

with (- - - -) & without stubs (——) at 5.2 GHz, with (- - - -) & without stubs (——) at 10.4 GHz and with(- - - -) & without stubs (——) at 15.05 GHz).

Figure 9. Measured 2D co-polar radiation patterns.

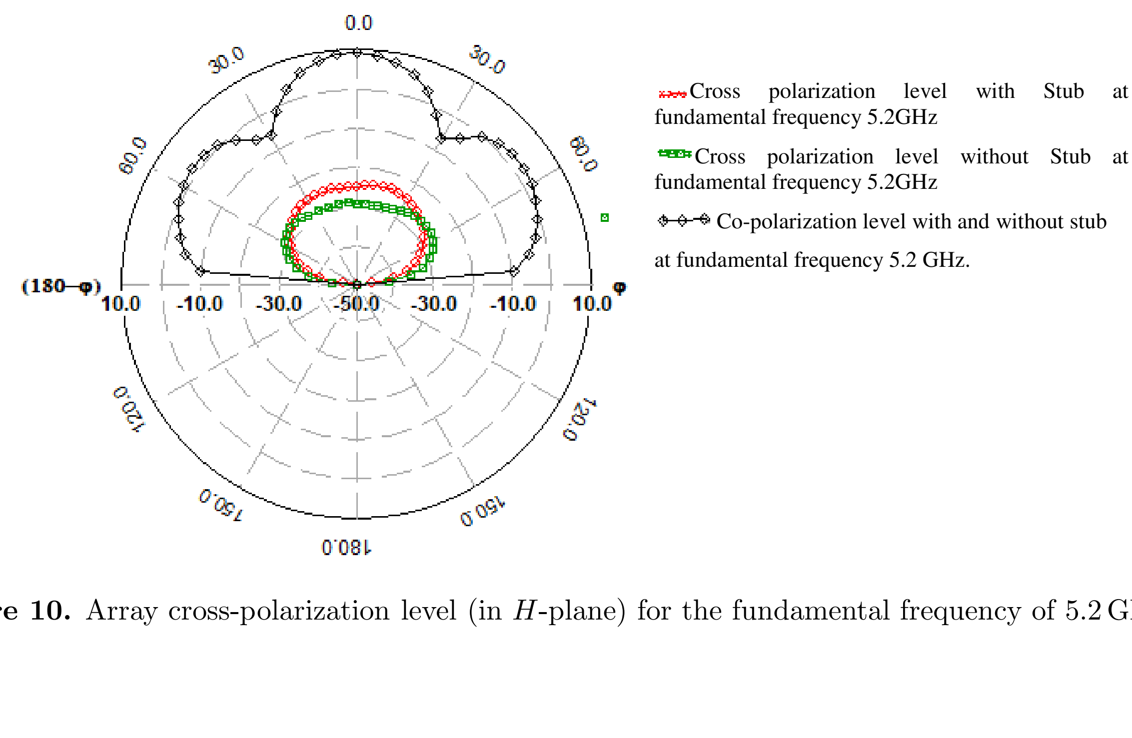

Figure 10. Array cross-polarization level (in H-plane) for the fundamental frequency of 5.2 GHz.

There is a significant difference between simulated and measured patterns at 15.05 GHz. The mismatch between the simulated and measured results has occurred due to probable imperfections in the fabrication process, coupled with the possible presence of unknown parasitic effects which was not considered in the simulation process. Furthermore, hand soldering of SMA connectors may have been one of the causes of the aforesaid discrepancy.

The array cross-polarization level (in H-plane) for the fundamental frequency is shown in Fig. 10. Here co-polarization is also given for the comparison. From Fig. 10, it is observed that cross-polarization level in H-plane is very low, and the difference between co-polarization and cross-polarization levels is 47 dB. It has been observed after implementing the stub that the cross-polarization level has been increased slightly, but it is within the accepted level.

4. CONCLUSION

The higher order modes (TM_{01}, TM_{11}, TM_{20}, TM_{12}, and TM_{30}) of fundamental frequency (TM_{10}) are successfully suppressed in microstrip antenna array. A pair of microstrip stubs of electrical length $\lambda_{g1}/2$, each (stub-A) placed on both sides of the feed line, results in reduction of the 1st harmonic along with some other adjacent sub-harmonics. Similarly, a pair of T-shaped stubs (stub-B) of electrical length $\lambda_{g2}/4$, each placed on both sides of the microstrip feed line, results in suppression of the 2nd harmonic along with a few other sub-harmonics. When both stubs (stub-A & stub-B) are simultaneously integrated with the feed line of the array, the harmonic signals existing in between 6–16 GHz are fully suppressed. In the present design, higher order modes are controlled by stubs only, and the limitation of the DGS or PBG structure has been overcome without degrading other parameters of antenna array. The utility of the proposed design lies in its use for WLAN applications.

REFERENCES

1. Garg, R., P. Bhartia, I. Bahl, and A. Ittipiboon, *Microstrip Antenna Design Handbook*, Artech House, Norwoord, 2000.
2. Horri, Y. and M. Tsutsumi, "Harmonic control by photonic bandgap on microstrip patch antenna," *IEEE Microwave Guided Letters*, Vol. 9, 13–15, 1999.
3. Chandra, U., H. F. AbuTarboush, H. S. Al-Raweshidy, and R. Nilavalan, "Wideband slotted patch antennas using EBG structures," *International Workshop on Antenna Technology (iWAT)*, May 13, 2010.
4. Biswas, S., D. Guha, and C. Kumar, "Control of higher harmonics and their radiations in microstrip antennas using compact defected ground structures," *IEEE Transaction on Antennas and Propagation*, Vol. 61, 3349–3353, 2013.
5. Ghosh, C. K., "Harmonic suppression of microstrip antenna by using open ended stubs," *Microwave and Optical Technology Letters*, Vol. 58, No. 6, 1340–1345, 2016.
6. Das Chagas Barbosa de Sena, F. and J. P. da Silva, "Harmonic suppression using optimised hexagonal defected ground structure by genetic algorithm," *IET Microwaves, Antennas & Propagation*, Vol. 12, No. 10, 1645–1648, 2018.
7. Elsheakh, D. N., M. F. Iskander, E. A. Abdallah, H. A. Elsadek, and H. Elhenawy, "Microstrip array antenna with new 2d-electromagnetic band gap structure shapes to reduce harmonics and mutual coupling," *Progress In Electromagnetics Research C*, Vol. 12, 2010.
8. Pandhare, R. A., P. L. Zade, and M. P. Abegaonkar, "Harmonic control by defected ground structure on microstrip antenna array," *Indian Journal of Science and Technology*, Vol. 8, No. 35, December 2015.
9. Pattapu, U., A. Gupta, and S. Das, "A 2.45 GHz harmonic suppression array antenna for rectenna application," *3rd International Conference on Microwave and Photonics*, February 2018.
10. Zhang, H., X.-Y. Huang, and H.-Y. Xu, "Spurious modes reduction in a patch antenna using an EBG-based microstrip transmission line filter," *Progress In Electromagnetics Research C*, Vol. 25, 41–54, 2012.

11. Abbasiniazare, S., K. Forooraghi, A. Torabi, and O. Manoochehri, "Mutual coupling compensation for a 1×2 short helical antenna array using split-ring resonators," *Electromagnetic Waves and Applications (Taylor* & *Francis)*, Vol. 33, 1–9, DOI: 10.1080/02726343.2013.751005, 2013.
12. Balanis, C. A., *Antenna Theory: Analysis and Design*, 4th edition, John Wiley, Hoboken, NJ, 2016.